Electric-Field Generation by Gas–Solid Combustion

K. S. Martirosyan, I. A. Filimonov, and Dan Luss
Dept. of Chemical Engineering University of Houston, Houston, TX 77204

The combustion of metal particles may generate a temporal electrical field due to a difference in the electrochemical potential across the growing oxide shell, which usually is a mixed ionic electronic conductor. A novel measurement technique enables simultaneously measurement of the temporal electrical field and temperature generated by a planar reaction wave during highly exothermic gas–solid reactions. The voltage formed after the rate of the temperature rise reached its maximum value, but before the temperature attained its maximum. For both simple (TiO_2, Fe_2O_3, MgO) and complex oxides ($LiMn_2O_4$, $SrFe_{12}O_{19}$, $PbFe_{12}O_{19}$, $BaTiO_3$) the voltage grew to its maximum value within 0.2–0.6 s, irrespective of the distance between the measuring probes. The decay of the voltage signal was slower than its rise. Increasing the distance between the measuring probes increased the period during which the voltage decayed. The difference between the time at which the temperature attained its maximum and the electrical signal vanished depended on both the distance between the two probes, and on the difference in time at which the voltage and temperature attained their maximum. Changing the exothermicity of the reaction (by dilution of the reactant mixture) can shift the time of the voltage decay relative to that at which the maximum temperature occurs. © 2004 American Institute of Chemical Engineers *AIChE J,* 50: 241–248, 2004
Keywords: metal combustion; temperature wave; double layer; induced electric potential; temperature-voltage relation

Introduction

A gradient in the electrochemical potential, which consists of both the chemical and electrical potentials, is the driving force for charge and mass transfer in electrolytes (Nernst, 1888; Debye, 1917). During metal oxidation a temporal difference in the electrochemical potential develops across the growing metal oxide layer, which is usually a mixed ionic electronic conductor. This led to early predictions that an electric field may form during gas–solid reaction (Wagner, 1930, 1933, 1975; Kroger and Vink, 1956; Kroger, 1964; Cabrera and Mott, 1949). While early studies considered charged species moving through the oxide in a pairwise manner (Wagner, 1930, 1933, 1975), current theories take into account movement of a set of charge carriers (Fromhold, 1976, 1980; Fromm, 1989; Kapila and Plawsky, 1993). Rode et al. (1995a,b) showed that the electrical field might affect the elastic stresses within the oxidized layer. The theoretical predictions were made assuming local electrochemical equilibrium inside the electrolyte and chemical equilibrium on the oxide surface. These assumptions are valid only at low oxidation temperatures having a characteristic time of the order of hours and days (Fromhold, 1976, 1980; Fromm, 1989; Kapila and Plawsky, 1993; Rode et al., 1995a,b). However, these assumptions and corresponding predictions are invalid during very fast, high-temperature reactions.

Several contactless measurements of the electromagnetic-field formation during self-propagating high-temperature synthesis (SHS) and metal oxidation have recently been reported. Maksimov et al. (2000) measured the transient magnetic field by coils surrounding the sample; Kudryashov et al. (1996)

Correspondence concerning this article should be addressed to D. Luss at dluss@uh.edu.
Current address of I. A. Filimonov: Institute of Structural Macrokinetics and Materials Science Russian Academy of Sciences, Chernogolovka, 142432, Russia.

© 2004 American Institute of Chemical Engineers

measured the electric field formed in the gas adjacent to the sample surface; Merzhanov et al. (1992) detected by fluxgate magnetometer the magnetic field formed in a ferromagnetic product; Nersesyan et al. (1999) and Claycomb et al. (2000) measured the temporal magnetic field by a superconducting quantum interference device (SQUID); and Morozov et al. (1996) and Nersesyan et al. (2001a,b, 2002) studied the electrical voltage generated inside the combusting sample between two electrodes separated by a distance (order of 6 mm) in the direction of the propagating front. A voltage signal was detected only when the first electrode was already in the post-combustion region, while the second was either in the pre-heated or in the reaction zone. The two electrodes were separated by regions with different temperatures, oxygen pressures, oxidation degrees, and electric resistances during the signal. The previous studies provided integral information about the electrical signal, its amplitude, and shape, but did not enable relating the local electrical field (or potential) to the temperature and conversion. Martirosyan et al. (2003a) recently conducted simultaneous measurements of the temporal electric potential and temperature during the combustion of large ($\Phi \sim 0.8$ mm) single Zr, Ti, Fe, and Ni particles.

Here we use a novel experimental technique, recently developed by Martirosyan et al. (2003b), for measuring simultaneously the local electrical field and temperature generated by a moving high-temperature wave during high-temperature gas–solid oxidation. The data obtained by this technique enabled us to determine the temperature at which local electrical voltage forms and decays, as well as the relation between the temporal voltage and the rate of heat generation and temperature. This novel information enhances our understanding of the rate processes generating the electrical field and will help formulate models predicting this phenomenon. While our experiments involve gas–solid reactions, the same experimental method can be used to study the electrical-field characteristics of either solid–solid or solid–liquid high-temperature reactions.

Experimental System and Procedure

The combustion of a loose powder sample, about 2–10 cm long, 35 mm wide, and 6–8 mm high, was conducted in a quartz reactor (10 cm ID, 25 cm long) fed by oxygen at a flow rate of 1–10 L/min. The relative density of the loose powder samples was 0.3–0.4. A transverse electric cell, shown in Figure 1, measured the temporal temperature and electric voltage in a plane perpendicular to the direction of the moving planar combustion front. It consisted of two platinum electrodes ($\Phi = 0.2$ mm) located in a cross section of the sample, so that a planar combustion front passed by both electrodes at the same time. The distance between the two electrodes, l, was much smaller than their distance from the wall in order to exclude the influence of the front distortion by the reactor wall. S-Type (Pt-Rh) micro-thermocouples ($\Phi \sim 10$ μm) placed between the two electrodes were used to measure the combustion temperature.

In most experiments the temporal temperature, voltage, and/or current were simultaneously measured during the combustion. The thermocouple signals and the electric voltage and/or current were measured and recorded by 8 channels measuring block of voltmeters and/or ammeters connected to an Omega Data Acquisition Board. The impedance during the

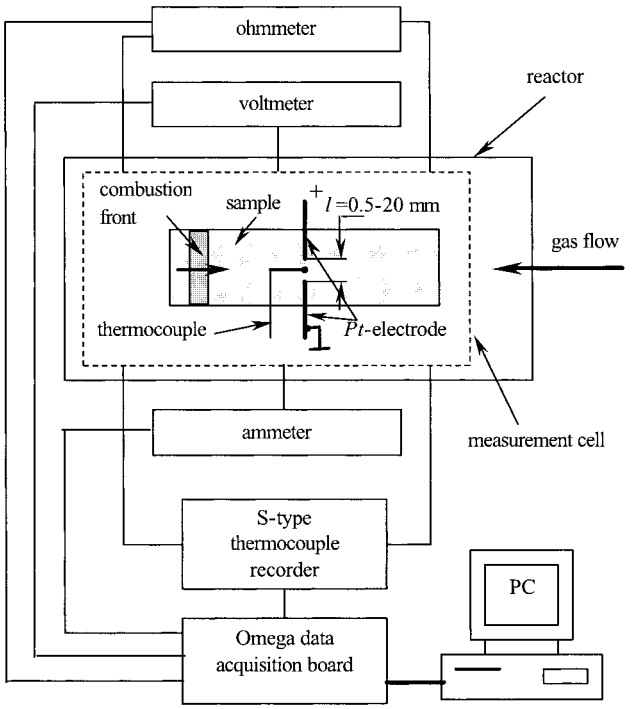

Figure 1. The experimental system.

voltage and current measurements was 0.25 MΩ and 0.1 Ω, respectively. The voltage signal was confirmed using an analog voltmeter with 2 MΩ internal resistance. The electric conductivity of the green charge and combustion products was measured by a digital ampere-voltmeter (Keithley Model 196 System DMM).

The reactive solid was diluted with the combustion product to keep the maximum temperatures in the range of 1050–1600°C to avoid melting. All the reactants and oxides used were 99+% pure (Sigma-Aldrich Chemical Company). The oxides were dried at 115°C for 5 h before the combustion and then mixed with the metal powder for 4 h in a ball mill (U.S. Stoneware, Mahwah, New York). The loose powder samples were placed in a 20-cm-long ceramic boat. A chemical match ($Ti + BaO_2 + Al_2O_3$) was used to initiate a planar combustion front.

Thermogravimetric (TG) and differential thermal analysis (DTA) by TG/DTA-320 thermo-analyzer (Seiko Instruments Inc.) were used to determine the temperatures at which the metal oxidation and various phase transformations occurred. An XRD (Siemens D-5000) was used to identify the combustion products. A digital video camera (Sony 3CCD) with a microscope (InfiniVar) was used to observe the shape of the combustion front.

Experimental Results

We measured simultaneously the temporal voltage and temperature in a plane parallel to the propagating reaction front during the combustion synthesis of simple and complex oxide products. Our experiments provided data about the temperature and time of voltage appearance, the duration of the signal rise and decay, and the voltage and current amplitudes during the synthesis. A digital camera indicated that the combustion on

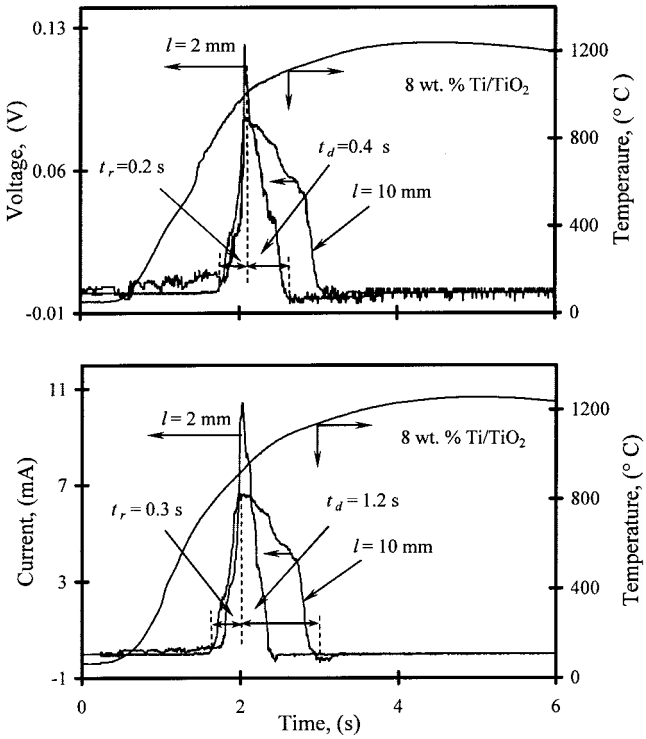

Figure 2. Temporal electric voltage, current, and temperature generated by a planar combustion front of Ti with distance/between electrodes.

the surface was planar. The thermocouples and electrodes were inserted at a depth of 1–2 mm from the surface and the electrodes were located a distance of 2 mm from each other. Thus, for the two electrodes the combustion front was planar, even if the front was somewhat distorted below the surface. Figure 2 shows the data obtained during the combustion of a mixture containing 8 wt % of titanium under oxygen flow rate of 8 L/min. The flow rate was measured at the atmospheric pressure and room temperature. This combustion occurred with the planar temperature front moving at a constant velocity of 0.85 mm/s. The electric voltage was measured between two probes separated by ~2 mm. It appeared at a temperature $T_i \sim$ 830°C. The maximum voltage ($V_{max} \sim 0.12$ V) and current (~10 mA) were attained at a temperature of ~1,000°C. The signal rise duration (t_r) was about 0.2 s and was always shorter than that of the signal decay ($t_d \approx 0.4$ s). Increasing the distance between the two probes did not affect t_r, but increased t_d and decreased the signal amplitude. The voltage was annihilated at a temperature of ~1,150°C, well before the maximum combustion temperature of 1,250°C was achieved. The electric resistance was about 15 Ω when the combustion front passed between the two probes. The cooled sample consisted of a loose uniform white powder. The thermogravimetric data showed that intense titanium oxidation began at 950°C. XRD analysis indicated that most of the Ti was converted to TiO_2 by the combustion. The observed maximum temperature was lower by about 500°C from the adiabatic temperature. The reason is that a large fraction of the conversion is completed by the slow postcombustion, during which the rate of heat loss exceeded that of the heat generation.

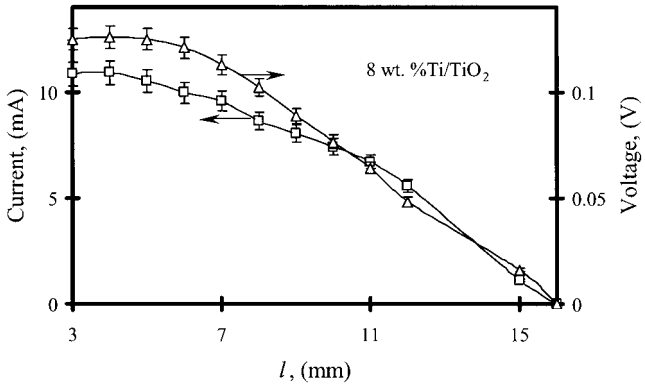

Figure 3. Dependence of the maximum voltage and current generated on the distance between the two electrodes, during combustion of Ti.

Experiments were conducted with a mixture containing 8 wt % Ti/TiO_2 to determine the impact of the distance between the two probes on the measured voltage and current (Figure 3). The largest voltage (current) amplitude of 0.13–0.14 V (~11 mA) was obtained when the distance between the probes (l) was ~3–4 mm and the signal vanished at a distance of 16 mm. In all these experiments the maximum voltage was obtained at about 1000°C and the signal vanished before the maximum temperature was reached.

The voltage generation during the combustion of a mixture containing 15 wt % Fe/Fe_2O_3 (Figure 4) started at a rather low temperature of 500°C. The maximum voltage ~0.07 V (current ~2.5 mA) was generated at a temperature of 705°C. The

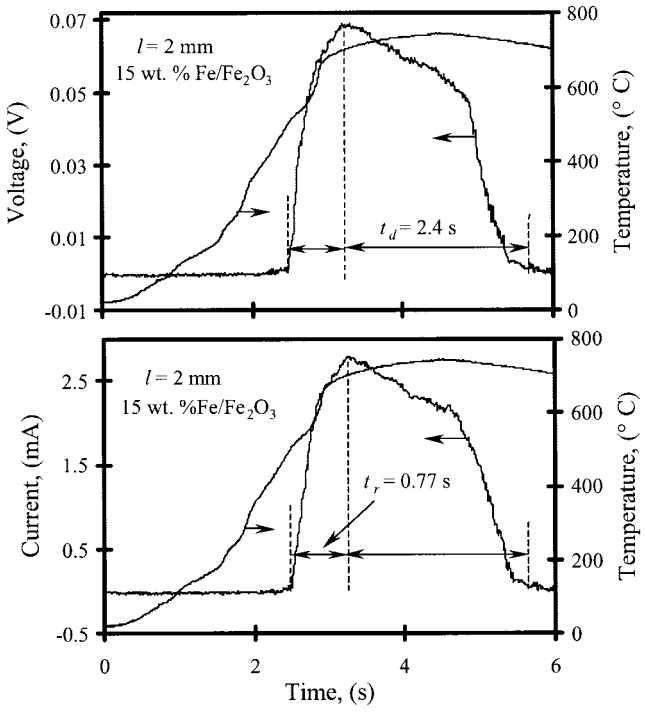

Figure 4. Temporal electric voltage, current, and temperature generated by a planar combustion of a mixture of 15 wt % Fe/Fe_2O_3.

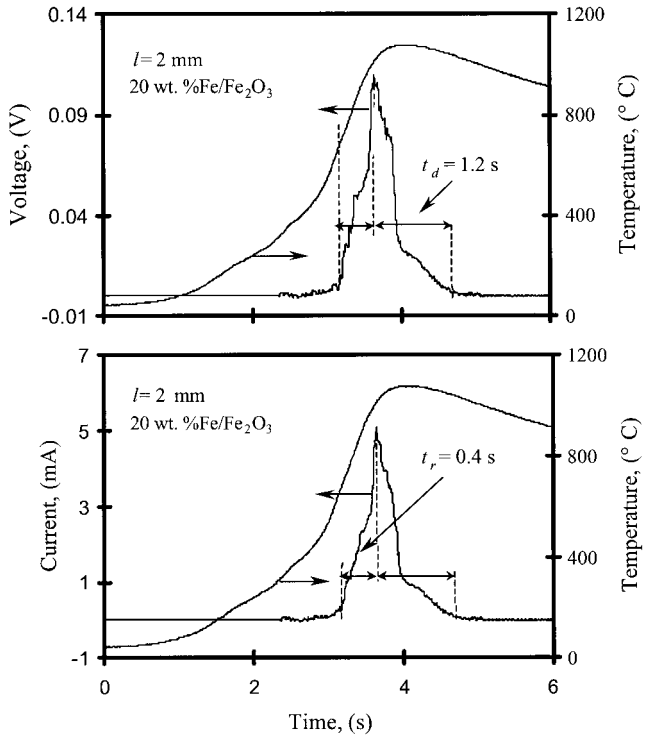

Figure 5. Temporal electric voltage, current, and temperature generated by a planar combustion of a mixture of 20 wt % Fe/Fe_2O_3.

electrical signal vanished after the maximum temperature was attained, that is, in the postcombustion zone. The duration of the signal rise ($t_r \approx 0.77$ s) and decay ($t_d \approx 2.4$ s) were longer than those for titanium.

An increase in the content of Fe in the green charge (Figures 4–6) increased the temperature at which the voltage generation started and that at which the maximum current was generated. It also increased the maximum combustion temperature and the voltage (current) amplitude. At the same time the increase in Fe content decreased the duration of the voltage rise and decay. Thus, for low Fe content (15–20 wt %), the electrical signal vanished after the maximum temperature was obtained, while for high Fe content (25 wt %), the signal vanished before this temperature was reached.

Table 1 reports the combustion velocity, temperature and key features of the electrical signal (temperature of voltage appearance, duration of the signal rise and decay, and voltage and current amplitudes) obtained during the following chemical reactions

$$Ti + TiO_2 + O_2 \rightarrow 2TiO_2 \quad (1)$$

$$2Fe + Fe_2O_3 + 1.5O_2 \rightarrow 2Fe_2O_3 \quad (2)$$

$$2Mg + MgO + O_2 \rightarrow 3MgO \quad (3)$$

$$Li_2O_2 + 2\,MnO_2 + 2Mn + O_2 \rightarrow 2LiMn_2O_4 \quad (4)$$

$$SrCO_3 + 3Fe_2O_3 + 6Fe + 4{,}5O_2 \rightarrow SrFe_{12}O_{19} + CO_2 \uparrow \quad (5)$$

$$PbO + 3Fe_2O_3 + 6Fe + 4.5O_2 \rightarrow PbFe_{12}O_{19} \quad (6)$$

$$2BaO_2 + TiO_2 + Ti \rightarrow 2BaTiO_3 \quad (7)$$

In all the reactions the maximum voltages and currents (0.1–0.52 V and 5–45 mA, respectively) were generated before the maximum combustion temperature (800–1150°C) was achieved. The maximum amplitude of the voltage signals obtained during the synthesis of the complex oxides ($PbFe_{12}O_{19}$, and $SrFe_{12}O_{19}$ or $BaTiO_3$) exceeded those generated during the synthesis of simple oxides (Fe_2O_3 or TiO_2). The characteristic duration of the signal rise was shorter than that of the signal decay. We did not observe any correlation between the combustion velocity or maximum combustion temperature and the amplitude of the electrical voltage or current. While the formation of some simple oxides (20 wt % Mg/MgO) produced very high temperatures but a small electric voltage, the synthesis of some complex oxides ($LiMn_2O_4$) generated a low combustion temperature and high current amplitude.

Discussion

The two electrodes, which were located in a plane normal to the direction of the propagating reaction front, were exposed to the same temporal temperature and conversion. The electrode ($\Phi \sim 200$ μm) and thermocouple diameters ($\Phi \sim 10$ μm) were

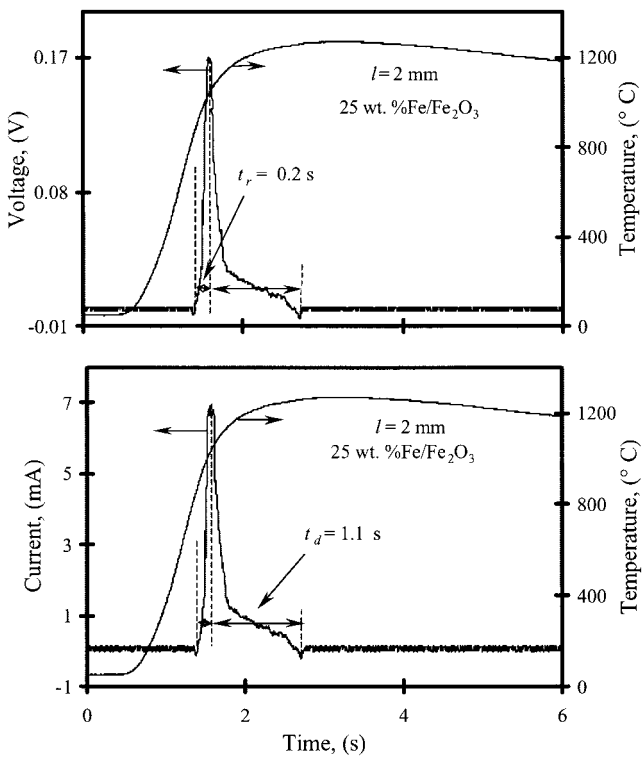

Figure 6. Temporal electric voltage, current, and temperature generated by a planar combustion of a mixture of 25 wt % Fe/Fe_2O_3.

Table 1. The Thermal-Wave Characteristics and Electric Signals Measured Along the Planar Combustion Front (distance between two electrodes 2 mm) in Different Mixtures

Mixture	Combustion Velocity (mm/s)	Maximum Combustion Temperature, T_{max} (°C)	Temperature and Time of the Voltage Appearance, °C (s)	Time of the Voltage		Temperature of the Signal Maximum, °C	Maximum Voltage (V)	Maximum Current (mA)
				Rise, t_r (s)	Decay, t_d (s)			
8 wt % Ti/TiO_2	0.85	1250	830, (1.4)	0.2	0.4	1000	0.12*	10
20 wt % Fe/Fe_2O_3	1.1	1100	700, (2.2)	0.4	1.2	1000	0.1	5
20 wt % Mg/MgO	3.6	1600	900, (1.4)	0.2	1.4	1150	0.52*	18
$LiMn_2O_4$	1.7	1200	650, (1.1)	0.2	1.2	980	0.42	45
$SrFe_{12}O_{19}$	1.1	1100	720, (2.7)	0.5	1.2	950	0.4*	10
$PbFe_{12}O_{19}$	1.2	1050	680, (2.1)	0.6	1.2	800	0.45*	15
$BaTiO_3$	1.6	1340	720, (1.9)	0.4	1.1	1000	0.5	20

*The signal vanishes before the maximum temperature.

much smaller than the width of the reaction front (~1 mm). Because the combustion was planar on the surface, it can be assumed that it was also planar between the two electrodes, which were separated by a distance of ~2 mm and inserted at about 1 mm below the surface. In contrast, when the electrodes were placed in the direction of the moving reaction front, they were separated by regions with different temperatures, oxygen pressures, oxidation degrees, and electric resistances during the signal. An important advantage of our measurements is that they enabled relating the measured signal to the local temperature and conversion.

The experiments revealed certain behavioral features of the electrical signal:

- The maximum voltage and current are generated well before the maximum combustion temperature has been attained;
- The electrical signal can vanish either before or after the maximum temperature is attained;
- The duration of the signal rise is shorter than that of its decay;
- The amplitude of the signal decreased with increasing distance between the two probes.
- Increasing the distance between the probes by a factor of about 5 had only a minor impact on the duration of the signal rise, but increased that of the decay.

In addition to the relation between the electrical signal and local temperature, it would be highly advantageous to know the local conversion. Unfortunately, the local conversion could not be measured *in situ* during the reaction. However, an approximate estimate of the relative reaction rate can be inferred by the ratio of the instantaneous temperature rise to its maximum value (that at the inflection point of the increasing temporal temperature). At low temperatures this ratio overestimates the reaction ratio, as part of the temperature rise is due to heat transfer from the approaching temperature front. At high temperatures the ratio underestimates the reaction ratio due to the heat loss to the atmosphere. However, this approximate ratio provides useful insight into the behavioral features of the electrical signal. Figures 7 and 8 show the temporal temperature and electric voltage generated during the combustion of Ti and Fe, as well as the ratio of the instantaneous temperature rise to the maximum one. In both cases the temperature rise occurred well before the voltage signal formed, and the growing oxide layer caused the reaction rate at the temperature maximum to be much smaller than that at the inflection point of the temperature profile.

The characteristic time of the oxygen ions diffusion, $t_{diff} \cong$

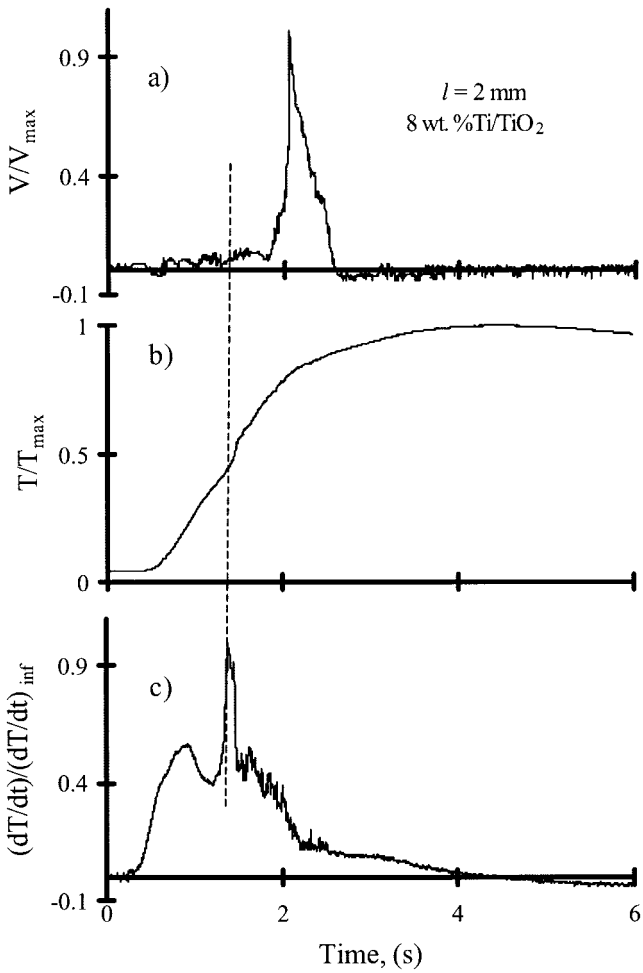

Figure 7. Temporal variation of the normalized (a) voltage generated; (b) local temperature; (c) temperature gradient by the combustion of a mixture of 8 wt % Ti/TiO_2, T_{max} ~ 1250°C, and V_{max} ~ 0.12 V.

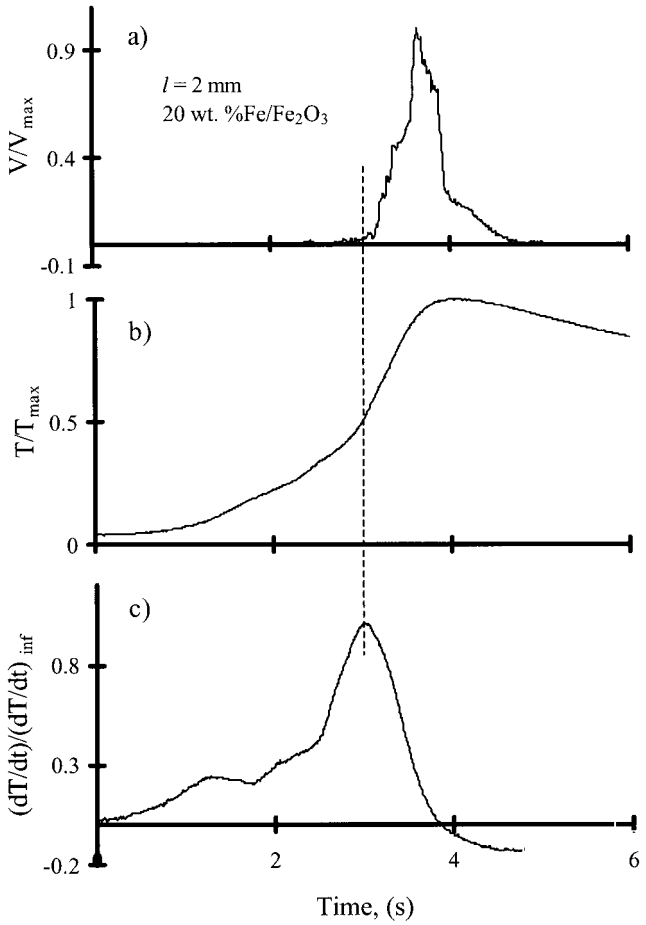

Figure 8. Temporal variation of the normalized: (a) voltage; (b) local temperature; (c) temperature gradient generated by the combustion of a mixture of 20 wt % Fe/Fe_2O_3, $T_{max} \sim 1100°C$, $V_{max} \sim 0.1$ V.

r^2/D_i, is much longer than that of the intrinsic metal oxidation, which is of the order of 1 ms at 500°C (Manning et al., 1997). For example, the diffusion of oxygen ions in titanium satisfies the relation

$$D_i = D_i^0 \exp(-E/RT), \tag{8}$$

with $D_i^0 \cong 1.6$ cm^2/s and $E = 202$ kJ/mole (Grigoriev and Melikhov, 1997). Thus, $D_i(1000°C) \cong 8.2 \times 10^{-9}$ cm^2/s and $D_i(1200°C) \cong 1.1 \times 10^{-7}$ cm^2/s. Thus, for typical titanium particles with $r \cong 5$ μm the characteristic diffusion time is of the order of 2–31 s. This long characteristic diffusion time causes the duration of the temperature rise and voltage signal to largely exceed that of the characteristic intrinsic reaction time.

At low temperatures the particles are heated by heat transfer from the approaching temperature front, and due to the low rate of the reaction and ion diffusion a double electric layer does not form. During this initial period both positive and negative charge carriers are produced on the particle surface. The sum of the surface positive and negative charges is very small due to the very low rate of diffusion of these carriers, that is, at most a very small voltage exists either on the surface or inside the particle.

As the particle heats up, the intrinsic reaction rate and the concentrations of the moving charge carriers increase rapidly. The slow rate of the oxygen ion diffusion becomes the rate-controlling step and the reaction proceeds by the shell progressive mechanism. The different rate of diffusion of the charge carriers across the growing oxide shell creates an electric double-charge layer. The production of positive and negative charge carriers (electron holes and oxygen ions, vacancies, and electrons), either on the reaction front and/or the particle surface, is a necessary but not sufficient condition for the generation of a voltage by the reaction. The formation of the electrical voltage and its polarity and amplitude depend on the difference in the diffusive velocity of the charge carriers. Thus, the diffusion processes limit the chemical reaction rate and determine the magnitude of the voltage.

The reaction rate and the corresponding rate of heat release attain their largest value in the vicinity of the inflection point of the temporal temperature. Due to the heat losses the inflection point differs slightly from the temperature of the maximum reaction rate. The subsequent decrease in heat generation is due to the increase in the thickness of the growing oxide layer. This decreases the diffusion rate of the oxygen ions, which is the reaction rate limiting step. Inspection of the ratio of the instantaneous temperature rise to its maximum value in Figures 7 and 8 clearly shows that the electrical signal forms in the region in which the reaction rate becomes appreciable. Its largest amplitude is attained closed to the time at which the temperature profile has an inflection point. For Fe (Ti) the temperature signal has an inflection at ~700°C (720°C). This occurred about 0.3 s (0.5 s) before the voltage attained its maximum value of ~0.1 V (0.12 V). The maximum temperature of ~1100°C (1250°C) was attained about 0.8 s (2 s) after the voltage reached its maximal value. While for Fe the reaction rate dropped sharply just before the maximum temperature was attained (~0.5 s), this occurred much earlier for Ti (~2 s).

Each experiment was repeated 10 times and the reproducibility of the electrical and temperature values was better than 10%. While this caused rather large deviations in the values of the time derivatives, it had a small impact on the times at which the maximum voltage was generated relative to those of the temperature inflection point and its maximum.

As the reaction rate becomes low (in the vicinity of the maximum temperature), almost uniform, quasi-equilibrium charge carrier distributions form throughout the particle and on the particle surface. The vanishing difference between the local positive and negative charges causes the voltage to decay.

The characteristic rise time of the signal depends on the carrier diffusion and chemical reaction rates and the rate of heat transfer from the approaching temperature front. It is, as Figure 2 shows, insensitive to changes in the distance between the measuring electrodes (one of which is the earth). In contrast, the characteristic time of the signal decay is strongly dependent on the distance between the two electrodes (Figure 2). It is well known that in an electrical circuit consisting of an inductance, resistance, and capacitance the decay time of the current grows with the resistance (Shire, 1960). The resistance between the two electrodes increases almost linearly with the distance between them. This increases the signal decay time upon increasing the distance between the probes. Figures 7 and 8 show that

at a constant distance of 2 mm, the decay time for both Fe and Ti was about 1 s. The specific electrical conductivities (per unit length) of both oxides at the corresponding maximum temperatures are of similar magnitude ($\sim 0.1\ \Omega^{-1}\ m^{-1}$).

Experiments with Fe mixtures showed that the relation between the time at which the electrical signal vanished and that at which the maximum temperature was attained depended on the dilution level of the Fe mixtures. At high dilution levels (Fe $\leq$ 20 wt %) the electrical signal vanished after the maximum combustion temperature was attained, while for more concentrated and exothermic mixtures (Fe $\geq$ 25 wt %) the electrical signal vanished before the maximum combustion temperature was attained. The increase in the reactant mixture exothermicity (i.e., Fe content) increased the difference between the time at which the maximum of reaction rate (voltage) was reached and that corresponding to the maximum combustion temperature. The increased Fe content also decreased the resistance between the electrodes which, in turn, decreased the signal decay duration.

We did not observe any correlation between the combustion velocity or maximum combustion temperature and the amplitude of the electrical signal. We noticed that the faster the maximum voltage was generated, the larger was the electric current amplitude (see Table 1). For simple oxides the diffusion coefficients of oxygen ion satisfy the inequality $D_i(\mathrm{Mg}) < D_i(\mathrm{Ti}) < D_i(\mathrm{Fe})$ ($D_i(1{,}000^\circ\mathrm{C}) \cong 1.75 \times 10^{-14}$ cm^2/s for MgO). It is possible that for slower ion diffusion coefficients the shell of oxide produced by the progressive shell mechanism forms at an earlier stage. This leads to a more rapid formation of the maximum electric voltage.

The decrease in the maximum voltage and current with distance between the two probes, shown in Figure 3, was caused by the increased resistance between the two probes. Preliminary experiments showed that it was not possible to reliably measure the voltage when the distance between the measuring probes was very small. The reason was that when the distance between the probes is of the order of the electrode diameter (0.2 mm), the measured voltage was affected and distorted by the earth electrode, which has always a zero electric potential.

Conclusions

The temporal voltage signal formed during the high-temperature gas–solid oxidation is due to a difference in the electrochemical potential across a growing metal oxide shell, which is usually a mixed ionic electronic conductor. The electric potential difference (an electric double-layer) is generated due to the different diffusive velocities of charge carriers across the oxide shell. The voltage signal formed after the temperature rise attained its maximal value and before the rising temperature reached its maximum. The voltage was generated only after an oxide shell formed with a sufficient difference in the fluxes of the positive and negative charges across it. Because the diffusion coefficients of the charge carriers have a very high activation energy, this occurred at relatively high temperatures. The growing shell thickness decreased the reaction rate and the flux of the charge carriers, leading to an eventual decay of the electrical signal.

The duration of the period during which the electrical signal increased was insensitive to changes in the distance between the measuring probes. We believe that this was due to the fact that the voltage evolution and increase depended only on the local reaction rate and the fluxes of the charge carriers. In contrast, the decay time of the electrical signal depended on the distance between the two probes. The reason is that the decay time of the voltage depended on the resistance in the circuit between the two probes, one of which was the earth.

The difference between the time at which the temperature attained its maximum and the electrical signal vanished depended on both the distance between the two probes, which affected the decay time, and on the difference in time at which the voltage and temperature attained their maximum. The data indicate that while in some cases the electrical signal decayed ahead of the time at which the temperature maximum was reached during the combustion of Ti, an inverse situation occurred during some of the Fe combustion experiments. It is of academic interest and potential practical value to develop *a priori* predictions of the magnitude and duration of the electrical signal.

The use of probes placed in a plane, perpendicular to the direction in which the combustion front propagated, enables relating the transient local temperature rise and voltage generated during high-temperature gas–solid oxidation. This measurement method provides information not attainable by using probes separated by a distance in the direction of the propagating combustion front.

Acknowledgment

We wish to acknowledge the financial support of this research by the National Science Foundation, U.S. Civilian Research and Development Foundation, and the Materials Research Science and Engineering Center at the University of Houston.

Literature Cited

Cabrera, N., and N. F. Mott, "Theory of the Oxidation of Metals," *Prog. Phys. Rep.,* **12,** 163 (1949).

Claycomb, J. R., W. LeGrand, J. H. Miller, Jr., M. D. Nersesyan, J. T. Ritchie, and D. Luss, "Chemomagnetic Characterization of Chemical Reactions Using High-T_c SQUIDs," *Phisica C,* **341,** 2641 (2000).

Debye, P., "Der Erste Electronenring der Atome," *Phys. Z.,* **18,** 276 (1917).

Fromm, E., "Model Calculations of Metal Oxidation at Ambient Temperatures," *Non-Stoichiometric Compounds, Surfaces, Grain Boundaries and Structural Defects,* J. Nowotny and W. Weppner, eds., Kluwer, New York, p. 523 (1989).

Fromhold, A. T., *Theory of Metal Oxidation (Defects in Crystalline Solids),* Vol. 1, North-Holland, Amsterdam, (1976).

Fromhold, A. T., *Theory of Metal Oxidation (Defects in Solids),* Vol. 2, North-Holland, Amsterdam (1980).

Grigoriev, I. S., and E. Z. Melikhov, *Handbook of Physical Quantities,* CRC Press, Boca Raton, p. 1548 (1997).

Kapila, D., and J. L. Plawsky, "Solid State Film Diffusion for the Production of Integrated Optical Waveguides," *AIChE J.,* **39,** 1186 (1993).

Kroger, F. A., and H. J. Vink, "Relations Between the Concentrations of Imperfections in Crystalline Solids," *Solid State Physics,* Vol. 3, F. Seitz and D. Turnbull, eds, Academic Press, New York, p. 307 (1956).

Kroger, F. A., *The Chemistry of Imperfect Crystals,* Wiley, New York (1964).

Kudryashov, V. A., A. S. Mukasyan, and I. A. Filimonov, "Chemoionization Waves in Heterogeneous Combustion Processes," *J. Mater. Synth. Process,* **4**(5), 353 (1996).

Maksimov, Yu. M., A. I. Kirdyashkin, V. S. Korogodov, and V. L. Polyakov, "Generation and Transfer of an Electric Charge in Self-Propagating High-Temperature Synthesis Using the Co-S System as an Example," *Combust. Explos. Shock Waves,* **36**(5), 130 (2000).

Manning, P. S., J. D. Sirman, R. A. DeSouza, and J. A. Kilner, "The

Kinetics of Oxygen Transport in 9.5 mol % Single Crystal Yttria Stabilised Zirconia," *Solid State Ionics,* **100,** 1 (1997).
Martirosyan, K. S., I. A. Filimonov, M. D. Nersesyan, and D. Luss, "Electric Field Formation during Combustion of Single Metal Particles," *J. Electrochem. Soc.,* **150**(5), 9 (2003a).
Martirosyan, K. S., I. A. Filimonov, and D. Luss, "New Measuring Techniques of Electric Field Generated by Combustion Synthesis," *Int. J. SHS.*, **11**(4), 325 (2003b).
Merzhanov, A. G., S. O. Mkrtchyan, M. D. Nersesyan, P. B. Avakyan, and K. S. Martirosyan, "Magnetic Field Caused by SHS Process," *Dokl. Akad. Nauk. RA,* **93**(2), 81 (1992).
Morozov, Y. G., M. V. Kuznetsov, M. D. Nersesyan, and A. G. Merzhanov, "Electrochemical Phenomena in the Processes of the SHS," *Dokl. Akad. Nauk. Rossii,* **351**(6), 780 (1996).
Nernst, W., "Zur Kinetik der in Losung Befindlichen Korper," *Z. Phys. Chem.,* **2,** 613 (1888).
Nersesyan, M. D., J. R. Claycomb, Q. Ming, J. H. Miller, J. T. Richardson, and D. Luss, "Chemomagnetic Fields Produced by Solid Combustion Reactions," *Appl. Phys. Lett.,* **75**(8), 1170 (1999).
Nersesyan, M. D., J. R. Claycomb, J. T. Ritchie, J. H. Miller, J. T. Richardson, and D. Luss, "Electric and Magnetic Fields Generated by SHS," *J. Mater. Synth. Process,* **9**(2), 63 (2001a).
Nersesyan, M. D., D. Luss, J. R. Claycomb, J. T. Ritchie, and J. H. Miller, Jr., "Magnetic Fields Produced by Combustion of Metals in Oxygen," *Combust. Sci. Technol.,* **169,** 89 (2001b).
Nersesyan, M. D., J. T. Ritchie, I. A. Filimonov, J. T. Richardson, and D. Luss, "Electric Fields Produced by High-Temperature Metal Oxidation," *J. Electrochem. Soc.,* **149**(1), J11 (2002).
Rode, H., D. Orlicki, and V. Hlavacek, "Reaction Rate Modeling in Noncatalytic Gas-Solid Systems: Species Transport and Mechanical Stress," *AIChE J.,* **41**(12), 2614 (1995a).
Rode, H., D. Orlicki, and V. Hlavacek, "Noncatalytic Gas-Solid Reactions and Mechanical Stress Generation," *AIChE J.,* **41**(5), 1235 (1995b).
Shire, E. S., *Classical Electricity and Magnetism,* Cambridge Univ. Press, Cambridge, p. 396 (1960).
Wagner, C., "Uber den Zusammenhang Zwischen Ionenbeweglichkeit und Diffusionsgeschwindigkeit in Festen Salzen," *Z. Phys. Chem.,* **B11,** 139 (1930).
Wagner, C., "Beitrag zur Theorie des Anlaufvorgangs," *Z. Phys. Chem.,* **B21,** 25 (1933).
Wagner, C., "Equations for Transport in Solid Oxides and Sulfides of Transition Metals," *Prog. Solid State Chem.,* **10**(1), 3 (1975).

Manuscript received Mar. 24, 2003, and revision received June 6, 2003.